Acta Crystallographica Section D
Biological Crystallography
ISSN 0907-4449

Crystallization and preliminary crystallographic investigations of avian 5-aminoimidazole-4-carboxamide ribonucleotide transformylase–inosine monophosphate cyclohydrolase expressed in *Escherichia coli*

Vicente M. Reyes,[a] Samantha E. Greasley,[a] Enrico A. Stura,[a]† G. Peter Beardsley[b] and Ian A. Wilson[a]*

[a]Department of Molecular Biology and the Skaggs Institute for Chemical Biology, The Scripps Research Institute, 10550 North Torrey Pines Road, La Jolla, CA 92037, USA, and [b]Departments of Pediatrics and Pharmacology, Yale University School of Medicine, 4083 LMP, 333 Cedar Street, PO Box 208064, New Haven, CT 06520-8064, USA

† Present address: Département d'Ingenierie et d'Etudes des Proteines, CEA, Saclay, France.

Correspondence e-mail: wilson@scripps.edu

Received 24 April 2000
Accepted 26 May 2000

ATIC [5-aminoimidazole-4-carboxamide ribonucleotide transformylase (AICAR Tfase)–inosine monophosphate cyclohydrolase (IMPCH)] is a bifunctional enzyme that catalyzes the penultimate and final steps in the *de novo* purine biosynthesis pathway and thus is an attractive anticancer target. Recombinant avian ATIC has been purified from an *Escherichia coli* expression system and crystallized in a binary complex with methotrexate (MTX). Crystals were obtained from PEG 4000 or MPEG 5000 buffered at pH 7.0–7.2 and data were collected from a single crystal at 96 K to 2.3 Å resolution at the Stanford Synchrotron Radiation Laboratory (SSRL). The crystals are monoclinic and belong to space group $P2_1$, with unit-cell dimensions a = 65.17, b = 105.93, c = 103.47 Å, β = 108.27°. Assuming two molecules per asymmetric unit, the Matthews coefficient V_m is 2.63 Å^3 Da^{-1} and the solvent volume is 52.9%.

1. Introduction

De novo purine biosynthesis is the biochemical pathway by which the purine ring is assembled through ten successive steps (Fig. 1) from 5-phosphoribosyl-1-pyrophosphate (PRPP; for a review, see Zalkin & Dixon, 1992). Two of these steps are folate-dependent (steps 3 and 9; Fig. 1) and involve the transfer of a formyl group from the cofactor 10-formyl-tetrahydrofolate (Mueller & Benkovic, 1981; Smith *et al.*, 1981) to the nascent purine ring. Specifically, step 3 is catalyzed by glycinamide ribonucleotide transformylase (GAR Tfase), while step 9, the transformylation of 5-aminoimidazole-4-carboxamide (AICAR) and 10-formyl-tetrahydrofolate to produce formyl-AICAR (FAICAR) and tetrahydrofolate (THF) is catalyzed by 5-aminoimidazole-4-carboxamide ribonucleotide transformylase (AICAR Tfase). AICAR Tfase represents only one activity of the 64.4 kDa bifunctional enzyme ATIC (also known as purH), which also possesses inosine monophosphate cyclohydrolase (IMPCH) activity (step 10; Fig. 1). Thus, ATIC catalyses the final two steps in the *de novo* purine biosynthesis pathway.

De novo purine and pyrimidine biosynthesis has been a long-term target for drug development for the treatment of human disorders such as cancer, autoimmune and inflammatory diseases and microbial infections. Two folate-dependent enzymes, thymidylate synthase (TS) and dihydrofolate reductase (DHFR), are proven targets for therapeutic strategies in the treatment of cancer; the crystal structures of these enzymes have been invaluable for furthering rational drug design (Appelt *et al.*, 1991; Hardy *et al.*, 1987; Schweitzer *et al.*, 1990). Clinically useful drugs such as methotrexate (MTX; Fig. 2; Chabner *et al.*, 1985), an anti-neoplastic and anti-inflammatory agent, and trimethoprim and pyrimethamine, both anti-infective agents, belong to a class of agents which are folate antagonists. An excellent understanding of the molecular basis of the mechanism of action of these folate antagonists has resulted from the three-dimensional structure determinations of enzyme–ligand complexes by X-ray crystallography (Matthews, Bolin, Burridge, Filman, Volz, Kaufman *et al.*, 1985; Matthews, Bolin, Burridge, Filman, Volz & Kraut, 1985; Reich *et al.*, 1992). Iterative cycles of design, synthesis, evaluation and crystallographic analysis have led to the development of a number of anti-cancer agents to the TS and DHFR targets (Appelt *et al.*, 1991; Webber *et al.*, 1993).

The discovery that 5,10-dideazatetrahydrofolate (DDATHF) selectively inhibited GAR Tfase, thus reducing *de novo* purine biosynthesis in both human and rodent tumors, identified this pathway as a viable target for

anti-neoplastic intervention (Beardsley *et al.*, 1989). The 6*R* diastereomer of DDATHF (lometrexol) has been used successfully in clinical trials as an antitumor agent (Erba *et al.*, 1994). The crystal structure of GAR Tfase has been determined in various apo and complexed forms (Almassy *et al.*, 1992; Chen *et al.*, 1992; Greasley *et al.*, 1999; Klein *et al.*, 1995; Su *et al.*, 1998) which have provided valuable insights into the mechanism of the formyl-transfer reaction. In addition, the crystal structures have aided in the design of more potent specific inhibitors to GAR Tfase, a number of which are presently being evaluated for potential clinical use (Boritzki *et al.*, 1996).

ATIC, like GAR Tfase, is also a prime target for rational drug design for anti-neoplastic intervention but has not been investigated as intensively as the other folate-dependent enzymes. The lack of identification of specific inhibitors of ATIC is in part a consequence of the lack of an available crystal structure of the enzyme to aid inhibitor design, despite the fact that both the prokaryotic and eukaryotic genes for ATIC have been cloned, expressed and purified (Ni *et al.*, 1991; Rayl *et al.*, 1996; Szabados *et al.*, 1994). Thus, the three-dimensional structure determination of ATIC and its utilization in the design of effective inhibitors could provide very welcome additions to the rather limited arsenal of anticancer agents.

In addition to its role in *de novo* purine biosynthesis, ATIC is involved in another biological process, that of inflammation, which has broad clinical significance (Baggott *et al.*, 1992). Low doses of MTX (Fig. 2) have been prescribed for the control of inflammation in rheumatoid arthritis and other inflammatory diseases (Cronstein *et al.*, 1993). Recent results indicate that the mechanism by which MTX controls inflammation is through its inhibition of the AICAR Tfase activity of ATIC, either directly as MTX-polyglutamate or indirectly from inhibition of DHFR (Allegra *et al.*, 1985; Baggott *et al.*, 1986; Cronstein *et al.*, 1993). Inhibition of AICAR Tfase activity leads to the accumulation of AICAR in the cell, which in turn results in increased levels of adenosine (as a result of AICAR's inhibitory properties on adenosine deaminase and/or adenosine kinase). The adenosine A2 receptors on neutrophils become saturated, which in turn impairs their capacity to adhere to endothelial cells and hinders invasion of the sites of inflammation, thus alleviating inflammatory symptoms (Gadangi *et al.*, 1996). The development of inhibitors to ATIC may therefore, through consideration of its crystal structure, lead to the treatment of both cancer and diseases associated with the anti-inflammatory response. Little is known about the mechanism of the formyl-transfer and cyclohydrolase reactions catalyzed by ATIC. Furthermore, sequence comparisons of various ATICs with all known protein sequences revealed no obvious homology, even to other folate-utilizing or AICAR-binding enzymes. The question then arises as to why these two functionalities, AICAR Tfase and IMPCH, exist on a single polypeptide chain and whether the FAICAR produced is channeled to the IMPCH active site. Truncation mutants of human ATIC have revealed that the AICAR Tfase and IMPCH activities exist in two independent domains (Beardsley *et al.*, 1998). The N-terminal region, residues 1–198, comprises the minimal domain for full IMPCH activity but no AICAR Tfase activity, while residues 199–591 have full AICAR Tfase activity but lack IMPCH activity. Hence, the crystal structure determination of ATIC is of great interest to further our mechanistic understanding and aid in the design of potent inhibitors of this key enzyme in the *de novo* purine biosynthesis pathway. Here, we present the purification, crystallization and preliminary X-ray analysis of avian ATIC in complex with MTX in order to set the stage for a complete structural determination of this important enzyme.

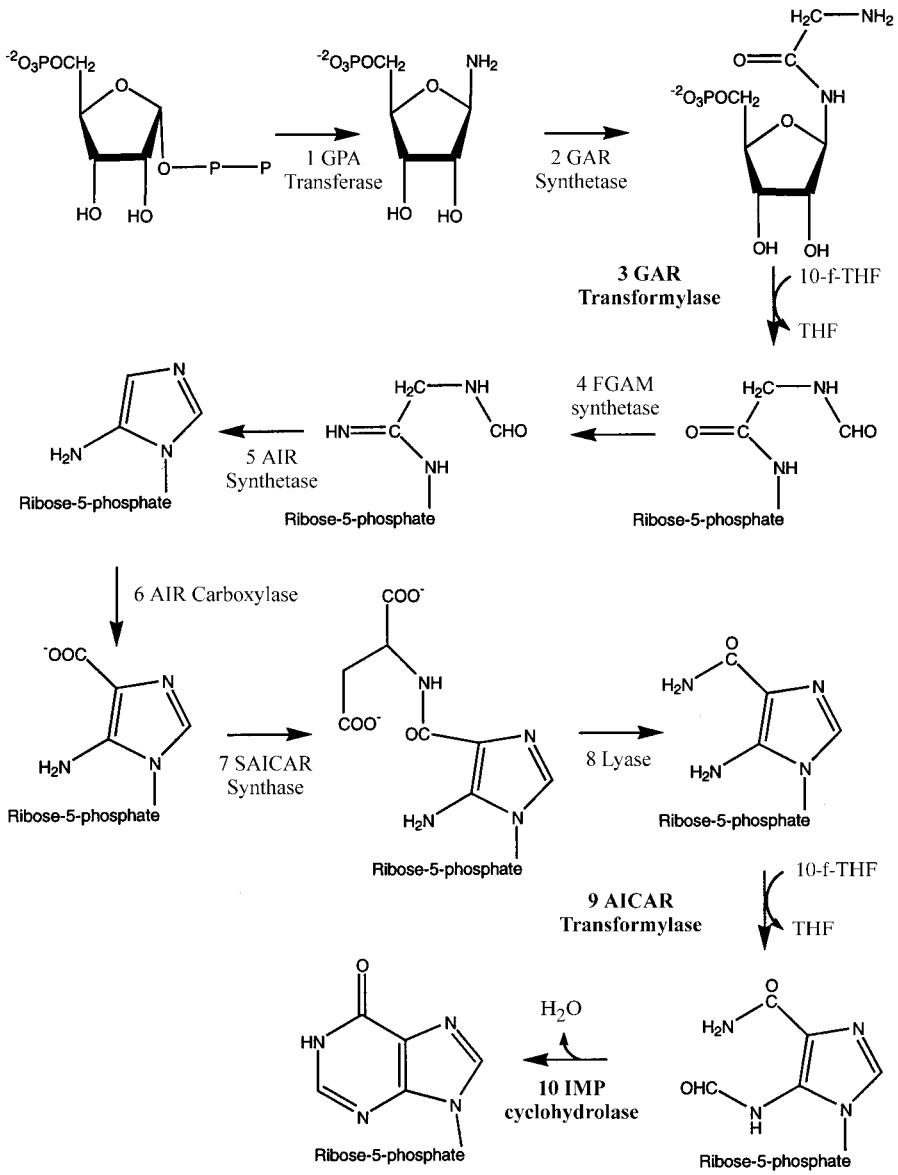

Figure 1
De novo purine-biosynthesis pathway.

Table 1
Data-collection statistics of avian ATIC in complex with MTX.

Numbers in parentheses refer to data in the highest resolution shell.

Space group	$P2_1$
Unit-cell parameters (Å, °)	a = 65.17, b = 105.93, c = 103.47, β = 108.27
Resolution (Å)	30–2.3 (2.38–2.30)
Total observations	132920
Unique reflections	54679
Multiplicity	2.4
Completeness (%)	89.8 (81.5)
Average $I/\sigma(I)$	10.6 (1.7)
$R_{\rm merge}$ (%)	8.1 (54.4)

2. Methods and results

2.1. Protein purification

The bacterial strain *E. coli* BL21.DE3 transformed with the plasmid pJC expressing avian ATIC as a C-terminal glutathione S-transferase (GST) fusion protein was grown in 1 l of 2YT media (Gibco BRL) at 310 K until an A_{600} of 0.6 was reached. Isopropyl-β-D-thiogalactopyranoside (Gibco BRL) was added to a final concentration of 500 µ*M* and incubation of the culture continued for an additional 5–6 h at 303 K. The cells were harvested by centrifugation at 2000*g* for 15 min at 277 K. The cell pellet was then resuspended in 10 ml PBST (20 m*M* sodium phosphate, 150 m*M* NaCl, 2 m*M* EDTA, 0.2 m*M* PMSF, 1% Triton X-100 pH 7.3) containing 0.1% β-mercaptoethanol, 100–200 units DNAase I and 15 mg ml^{-1} lysozyme. Cells were then sonicated at 277 K at 40% power for eight cycles of 15 s using a Virtis miniprobe. The cell lysate was clarified by centrifugation at 20 000*g* at 277 K for 60 min. The supernatant was subsequently added to 0.3–0.4 mg of GST-agarose beads and placed on a rotator for 2–3 h at 277 K. The GST-agarose beads were washed three times with PBST and then once with TCB (50 m*M* Tris, 150 m*M* NaCl, 2.5 m*M* $CaCl_2$ pH 8.0). The GST affinity tag was cleaved from the ATIC protein *in situ* by addition of thrombin to the bead slurry at a final concentration of 5 µg ml^{-1} and incubated at room temperature for 2–3 h. The beads were centrifuged at 1000*g* for 10 min and the ATIC protein was recovered in the supernatant (typically 5–10 mg of ATIC is obtained per liter of bacterial culture). Further purification and buffer exchange was performed on a size-exclusion column to remove small amounts of impurities using 0.33× TCB. Fractions were analyzed by SDS–PAGE and fractions containing ATIC were pooled. DTT was added to a final concentration of 0.4 m*M* and the protein was concentrated to 25–30 mg ml^{-1} for subsequent protein crystallization trials. For crystallization of the binary complex of ATIC and MTX, protein solution was prepared by addition of ligand in a powdered form to the dilute protein to a tenfold molar excess and incubation at 277 K for 1–2 h followed by filtration and concentration to 25–30 mg ml^{-1}.

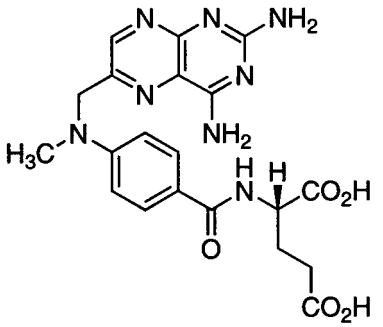

Figure 2
The folate-derived inhibitor methotrexate (MTX).

2.2. Crystallization

Initial crystals of ATIC were obtained from a footprint screen (Stura *et al.*, 1992), by the method of vapor diffusion in sitting drops at 295 K. However, nucleation could not be controlled, as observed from the showers of tiny crystals produced. As a result, further crystallization trials were performed under oil using the microbatch method (Blow *et al.*, 1994; Chayen, 1997; Chayen *et al.*, 1992). A droplet (typically 2–4 µl) containing ATIC in complex with MTX and precipitating solution as a 1:1 mixture was deposited into a well of a Terasaki plate (Hampton Research, Laguna Hills, CA, USA), which was previously filled with a thin layer of oil. The oil used was either light paraffin oil or 'Al's oil' (Hampton Research, Laguna Hills, CA, USA), which is a 1:1 mixture of light paraffin oil and silicone oil. Crystals can be grown from a precipitant solution of 18–24% monomethylether polyethylene glycol (MPEG) 5000 or PEG 4000, 0.4 m*M* DTT, 26 m*M* sodium thiocyanate and 100 m*M* HEPES or PIPES buffer pH 7.0–7.2. Crystallization under oil resulted in single crystals (0.3 × 0.2 × 0.1 mm) with fewer nucleation sites after 2–4 weeks at 295 K (Fig. 3). Crystallization conditions were refined with the Hampton Additive Screening Kits I and II (Hampton Research, Laguna Hills, CA, USA). The most useful additive was 5% glycerol, which allowed the crystals to be cryocooled for data collection without the requirement for further cryoprotectant.

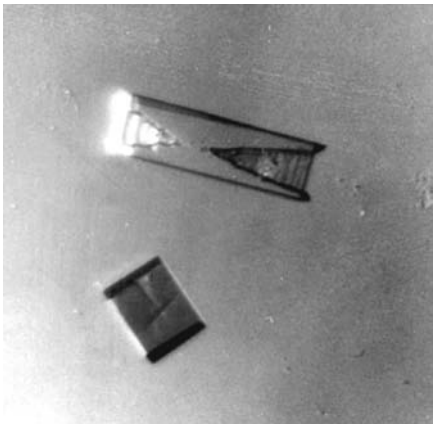

Figure 3
Crystals of avian ATIC in complex with MTX.

2.3. Data collection and processing

Data were initially collected in-house to 2.8 Å resolution at room temperature with a Hi-Star area detector mounted on a Siemens rotating-anode generator (Siemens Inc, Madison, WI, USA). Subsequently, data were collected from a single crystal to 2.3 Å resolution on beamline 7-1 at the Stanford Synchrotron Radiation Laboratory (SSRL). A suitable crystal, crystallized in the presence of 5% glycerol as a cryoprotectant, was mounted in a loop from Hampton Research by first removing all the oil surrounding the crystallization drop. The crystal was then flash-cooled in the nitrogen stream and a full data set collected at 96 K on a MAR Research imaging plate with a crystal-to-detector distance of 160 mm. Processing and scaling of the data (Table 1) was performed using the programs *DENZO* (Otwinowski, 1993) and *SCALEPAC*K (Otwinowski & Minor, 1997). The crystals belong to the space group $P2_1$, with unit-cell parameters a = 65.17, b = 105.93, c = 103.47 Å, β = 108.27°. It should be noted that the crystals can also be indexed in the orthorhombic space group $C222_1$, with unit-cell parameters a = 65.17, b = 196.50, c = 105.93 Å; however, data-collection statistics are poor ($R_{\rm merge}$ = 14.8% for $C222_1$ *versus* 8.1% for $P2_1$) and suggest that the crystals exhibit pseudo-symmetry. In addition, the data processed in the $P2_1$ space group were analyzed for higher metric symmetry and space-group determination with *XPREP* (Sheldrick, 1990–1995), which indicated the correct space group to be $P2_1$. A Matthews coefficient V_m (Matthews, 1968) of 2.63 Å^3 Da^{-1} is calculated, assuming two molecules in the asymmetric unit, with 52.9% solvent volume.

We are pursuing the structure determination of ATIC, either by isomorphous replacement or MAD, owing to the lack of a suitable search model for structure determination by molecular replacement.

This work was partially supported by NIH Grant CA63536 (IAW) and CA50721 (GPB). We thank Barbara Moroson and Dr Elizabeth Rayl of the Departments of Pediatrics and Pharmacology, Yale University School of Medicine, for protein purification and enzyme-activity assays, and Dr Mason Yamashita for help in the protein purifications and for useful discussions. This is publication 13200-MB from the Scripps Research Institute.

References

Allegra, C. J., Drake, J. C., Jolivet, J. & Chabner, B. A. (1985). *Proc. Natl Acad. Sci. USA*, **82**, 4881–4885.

Almassy, R. J., Janson, C. A., Kan, C. C. & Hostomska, Z. (1992). *Proc. Natl Acad. Sci. USA*, **89**, 6114–6118.

Appelt, K., Bacquet, R. J., Bartlett, C. A., Booth, C. L., Freer, S. T., Fuhry, M. A., Gehring, M. R., Herrmann, S. M., Howland, E. F., Janson, C. A., Jones, T. R., Kan, C.-C., Kathardekar, V., Lewis, K. K., Marzoni, G. P., Matthews, D. A., Mohr, C., Moomaw, E. W., Morse, C. A., Oatley, S. J., Ogden, R. C., Reddy, M. R., Reich, S. H., Schoettlin, W. S., Smith, W. W., Varney, M. D., Villafranca, J. E., Ward, R. W., Webber, S., Webber, S. E., Welsh, K. M. & White, J. (1991). *J. Med. Chem.* **34**, 1925–1934.

Baggott, J. E., Morgan, S. L., Ha, T., Vaughn, W. H. & Hine, R. J. (1992). *Biochem. J.* **282**, 197–202.

Baggott, J. E., Vaughn, W. H. & Hudson, B. B. (1986). *Biochem. J.* **236**, 193–200.

Beardsley, G. P., Moroson, B. A., Taylor, E. C. & Moran, R. G. (1989). *J. Biol. Chem.* **264**, 328–333.

Beardsley, G. P., Rayl, E. A., Gunn, K., Moroson, B. A., Seow, H., Anderson, K. S., Vergis, J., Fleming, K., Worland, S., Condon, B. & Davies, J. (1998). *Adv. Exp. Med. Biol.* **431**, 221–226.

Blow, D. M., Chayen, N. E., Lloyd, L. F. & Saridakis, E. (1994). *Protein Sci.* **3**, 1638–1643.

Boritzki, T. J., Barlett, C. A., Zhang, C. & Howland, E. F. (1996). *Invest. New Drugs*, **14**, 295–303.

Chabner, B. A., Allegra, C. J., Curt, G. A., Clendeninn, N. J., Baram, J., Koizumi, S., Drake, J. C. & Jolivet, J. (1985). *J. Clin. Invest.* **76**, 907–912.

Chayen, N. E. (1997). *Structure*, **5**, 1269–1274.

Chayen, N. E., Shaw Stewart, P. D. & Blow, D. M. (1992). *J. Cryst. Growth*, **112**, 176–180.

Chen, P., Schulze-Gahmen, U., Stura, E. A., Inglese, J., Johnson, D. L., Marolewski, A., Benkovic, S. J. & Wilson, I. A. (1992). *J. Mol. Biol.* **227**, 283–292.

Cronstein, B. N., Naime, D. & Ostad, E. (1993). *J. Clin. Invest.* **92**, 2675–2682.

Erba, E., Sen, S., Sessa, C., Vikhanskaya, F. L. & D'Incalci, M. (1994). *Br. J. Cancer*, **69**, 205–211.

Gadangi, P., Longaker, M., Naime, D., Levin, R. I., Recht, P. A., Montesinos, M. C., Buckley, M. T., Carlin, G. & Cronstein, B. N. (1996). *J. Immunol.* **156**, 1937–1941.

Greasley, S. E., Yamashita, M. M., Cai, H., Benkovic, S. J., Boger, D. L. & Wilson, I. A. (1999). *Biochemistry*, **38**, 16783–16793.

Hardy, L. W., Finer-Moore, J. S., Montfort, W. R., Jones, M. O., Santi, D. V. & Stroud, R. M. (1987). *Science*, **235**, 448–455.

Klein, C., Chen, P., Arevalo, J. H., Stura, E. A., Marolewski, A., Warren, M. S., Benkovic, S. J. & Wilson, I. A. (1995). *J. Mol. Biol.* **249**, 153–175.

Matthews, B. W. (1968). *J. Mol. Biol.* **33**, 491–497.

Matthews, D. A., Bolin, J. T., Burridge, J. M., Filman, D. J., Volz, K. W., Kaufman, B. T., Beddell, C. R., Champness, J. N., Stammers, D. K. & Kraut, J. (1985). *J. Biol. Chem.* **260**, 381–391.

Matthews, D. A., Bolin, J. T., Burridge, J. M., Filman, D. J., Volz, K. W. & Kraut, J. (1985). *J. Biol. Chem.* **260**, 392–399.

Mueller, W. T. & Benkovic, S. J. (1981). *Biochemistry*, **20**, 337–344.

Ni, L., Guan, K., Zalkin, H. & Dixon, J. E. (1991). *Gene*, **106**, 197–205.

Otwinowski, Z. (1993). *DENZO*. Yale University, New Haven, Connecticut, USA.

Otwinowski, Z. & Minor, W. (1997). *Methods Enzymol.* **276**, 307–326.

Rayl, E. A., Moroson, B. A. & Beardsley, G. P. (1996). *J. Biol. Chem.* **271**, 2225–2233.

Reich, S. H., Fuhry, M. A., Nguyen, D., Pino, M. J., Welsh, K. M., Webber, S., Janson, C. A., Jordan, S. R., Matthews, D. A., Smith, W. W., Bartlett, C. A., Booth, C. L. J., Herrmann, S. M., Howland, E. F., Morse, C. A., Ward, R. W. & White, J. (1992). *J. Med. Chem.* **35**, 847–858.

Schweitzer, B. I., Dicker, A. P. & Bertino, J. R. (1990). *FASEB J.* **4**, 2441–2452.

Sheldrick, G. M. (1990–1995). *XPREP*. Siemens Industrial Automation Inc., Madison, WI, USA.

Smith, G. K., Mueller, W. T., Benkovic, P. A. & Benkovic, S. J. (1981). *Biochemistry*, **20**, 1241–1245.

Stura, E. A., Nemerow, G. R. & Wilson, I. A. (1992). *J. Cryst. Growth*, **122**, 273–285.

Su, Y., Yamashita, M. M., Greasley, S. E., Mullen, C. A., Jennings, P. A., Warren, M. S., Benkovic, S. J. & Wilson, I. A. (1998). *J. Mol. Biol.* **281**, 485–499.

Szabados, E., Hindmarsh, E. J., Phillips, L., Duggleby, R. G. & Christopherson, R. I. (1994). *Biochemistry*, **33**, 14237–14245.

Webber, S. E., Bleckman, T. M., Attard, J., Deal, J. G., Kathardekar, V., Welsh, K. M., Webber, S., Janson, C. A., Matthews, D. A., Smith, W. W., Freer, S. T., Jordan, S. R., Bacquet, R. J., Howland, E. F., Booth, C. L. J., Ward, R. W., Herrmann, S. M., White, J., Morse, C. A., Hilliard, J. A. & Bartlett, C. A. (1993). *J. Med. Chem.* **36**, 733–746.

Zalkin, H. & Dixon, J. E. (1992). *Prog. Nucleic Acid Res. Mol. Biol.* **42**, 259–87.